Double Bethe lattice

Alexander E. Lukyanov,[1,2] Vyacheslav D. Neverov,[1,2] Yaroslav V. Zhumagulov,[1,2]
Andrey V. Krasavin,[1] Alexey P. Menushenkov,[1] and Alexei Vagov[2,3]

[1] *National Research Nuclear University MEPhI, Kashirskoye shosse 31, Moscow, 115409, Russian Federation*
[2] *ITMO University, Kronverksky Pr. 49, St. Petersburg, 197101, Russian Federation*
[3] *Institute for Theoretical Physics III, University of Bayreuth, Bayreuth 95440, Germany*

(Dated: April 27, 2020)

An article usually includes an abstract, a concise summary of the work covered at length in the main body of the article.

I. INTRODUCTION

[Pump-probe (PP) experiments and relaxation of excited state]

[Numerical modeling of PP]

[CDW, BaBiO3 and electron-phonon interaction]

[Target: possible XFEL experiments?]

[Model system: double Bethe lattice; previous results of PRB 59, 6846 (1999) and Lichtenstein]

[The aim of paper]

A. $BaBiO_3$-based compounds

Perovskite compounds based on $BaBiO_3$ are special representatives of the high-temperature superconductor (HTSC) class, which do not include transition metal ions. Superconductivity in these compounds with transition temperatures $T_c = 13K$ at doping with lead and $T_c = 34K$ at doping with potassium was discovered in 1975 [1] and in 1988 [2], respectively. Compounds belonging to the class of perovskites, as a rule, have a complex phase diagram, which includes dielectric – metal phase transitions and various structural phases when the degree of doping or temperature changes [3]. The parent compound of bismuthates $BaBiO_3$ is characterized by charge ordering, and has a transport gap of 0.25 eV [4], the origin of which is assumed to be associated with the "breathing distortion" phenomenon, when the sizes of BiO_6 octahedra alternate along three crystallographic directions with the formation of Bi–O bonds of various lengths [3]. This breathing mode is usually interpreted as the phenomenon of "disproportionation of valence" of Bi^{4+} [5] and the formation of ions Bi^{3+} and Bi^{5+}, which determine the different sizes of octahedra [6].

The presence of a number of extraordinary properties of bismuth-based HTSC, such as the existence of two energy gaps, transport and optical, differing in values by an order of magnitude; low density of states at the Fermi level; the manifestation of diamagnetism at any concentrations of dopants [7], gave impetus to numerous studies of these compounds, both experimental and theoretical, which have started more than thirty years ago and are currently ongoing. There is still no clear answer to the question of what causes the appearance of HTSC in $BaBiO_3$-based compounds. Recent experiments using the ARPES technique [8, 9] suggested that the generally accepted scenario of the disproportionation of valence may not be sufficiently correct, and the bismuth atoms that are part of octahedra of different sizes have the same valence. This assumption, however, has a serious counter-argument, expressed as early as 1996 in [10], in which a precise measurement of the photoemission X-ray spectra (XPS spectra) of $Ba_{1-x}K_xBiO_3$ single crystals was performed, indicating the presence of two different values of Bi$4f$ bond energies in doped $Ba_{1-x}K_xBiO_3$, which convincingly proves the existence of two different bismuth states in the compounds under study.

In [11–13], based on the results of experimental studies of X-ray absorption spectroscopy (XAS) [14, 15], a new description of the local electronic structure of bismuth-based HTSCs in the form of a spatially separated Fermi-Bose mixture was presented: two types of charge carriers, local electron pairs (bosons) and free electrons (fermions) coexist in $BaBiO_3$ doped with potassium with a concentration of $x \geq 0.37$. In this case, electron pairs participate in charge transfer and in the formation of superconductivity, while free electrons are responsible for the observed dielectric – metal phase transition and the appearance of a Fermi-liquid state when overcoming the percolation threshold ($x \geq 0.37$). It was suggested that the ground state exists in the $BaBiO_3$ compound in the form of a pair-charge-density wave (PDW) [13].

The understanding of the nature of the ground state of $BaBiO_3$ and, consequently, the explanation of properties of this compound, may be achieved by performing a pump-probe experiment on the excitation of the $BaBiO_3$ sample over the optical gap.

B. Pump-probe experiments

The technique of a pump-probe experiment is a valuable tool to study the interplay between microscopic degrees of freedom in correlated materials. In this technique, the pump pulse drives a system under study into a nonequilibrium state, the process which is often accompanied by a change in the phase state of the system. Afterwards, the second, probe pulse, monitors the response of the system to the pump pulse and its return to the

equilibrium state by varying the time delay between the pump and the probe.

The great progress in the pump-probe technique in recent decades has made it possible to discover many new phenomena in quantum materials [16, 17]. In the context of this study, we would like to note the particular success of the pump-probe technique in the study of cuprate superconductors [18–25], iron-based superconductors [26–29], and charge density wave (CDW) materials [30–36].

In the lattice of $BaBiO_3$ the neighboring BiO_6 octahedra are not equivalent. Slightly bigger octahedra have an electron pair on the upper antibonding Bi6s-O2p$_{\sigma^*}$ orbital, while smaller octahedra have a hole pair. The different electron filling of the Bi6s-O2p$_{\sigma^*}$ orbital of the neighboring BiO_6 octahedral complexes leads to the formation of a dynamical double-well potential for the vibration of oxygen ions, which arises due to the local electron pair tunneling between the neighboring octahedra; this potential was experimentally observed in EXAFS spectra [14, 15].

Ultrafast excitation over the optical gap will break the electron pair on the antibonding orbital and will cause the single electron to skip from the BiO_6 octahedron to the neighboring one with the hole pair, so that two different BiO_6 complexes turn into two similar ones with the accompanying removal of the lattice distortion (Fig. 1). Such an electronic structure change, as well as strong local deformation of the lattice and the appearance of local magnetic moment in the newborn BiO_6 complexes, may be probed with a spectroscopy technique. The characteristic times of relaxation after laser excitation are of the order of few ps [37].

C. The aim of the paper

II. MODEL

[double Bethe lattice]
[Modeling of the pump laser: hoppings modulation]
[Approximations used]
[Variables of interest]

The electron-phonon Hamiltonian on the double Bethe lattice reads:

$$H = \left(-t_{\parallel} \sum_{\langle i,j\rangle \alpha\sigma} c^{\dagger}_{j\alpha\sigma} c_{i\alpha\sigma} - t_{\perp} \sum_{i\sigma} c^{\dagger}_{i1\sigma} c_{i2\sigma} + \text{h.c.} \right) - \mu \sum_i n_i + g \sum_i \left(b^{\dagger}_i + b_i \right) (n_i - 1) + \omega_0 \sum_i b^{\dagger}_i b_i. \quad (1)$$

Here $\langle i,j\rangle$ denotes nearest-neighbor lattice sites; σ is the spin; $\alpha = 1, 2$ is the Bethe lattice index; $c^{\dagger}_{i\sigma}$ ($b^{\dagger}_i$) is the creation operators of an electron (phonon); μ is the chemical potential; g is the constant of the electron-phonon coupling; ω_0 is the phonon frequency. The amplitudes $t_{\parallel}$ and $t_{\perp}$ are hopping parameters within and between Bethe lattices, respectively (the symbol $t_{\parallel}$ is used to avoid confusion with the time variable t); $n_i = n_{i\uparrow} + n_{i\downarrow}$.

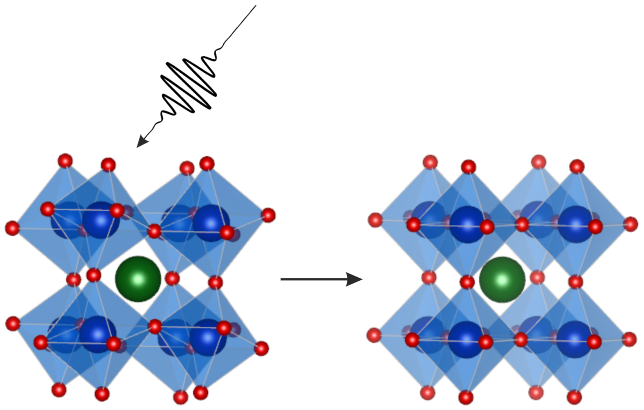

FIG. 1. The effect of a pump laser on $BaBiO_3$ lattice. The excitation over the optical gap breaks electron pairs on the upper antibonding Bi6s-O2p$_{\sigma^*}$ orbital, leading to the removal of lattice distortions and the appearance of a magnetic moment on BiO_6 octahedra. Bismuth, oxygen, and barium atoms are shown in blue, red, and green, respectively.

In the DMFT approach [38], the lattice problem (1) is mapped to an effective impurity model, which in our case is a dimer, connected to a free electron bath characterized by the hybridization function $\Delta(t,t')$ (defined below). The effective action of the impurity model is

$$\mathcal{S}_{\text{imp}} = i \sum_{\sigma} \int_{\mathcal{C}} dt dt'\, c^{\dagger}_{\sigma}(t) \mathcal{G}_0^{-1}(t,t') c_{\sigma}(t') + i \int_{\mathcal{C}} dt dt'\, X(t) \frac{D_0^{-1}(t,t')}{2} X(t') - ig \sum_{\sigma} \int_{\mathcal{C}} dt\, X(t) c^{\dagger}_{\sigma}(t) c_{\sigma}(t), \quad (2)$$

where the intergation is performed along the Kadanoff–Baym (KB) contour $\mathcal{C}$ (Fig. 2); $X = b^{\dagger} + b$; $\mathcal{G}_0(t,t')$ is the Weiss Green's function (GF) for the impurity model, which is related to the hybridization function by

$$\mathcal{G}_0^{-1}(t,t') = [i\partial_t + \mu]\, \delta_{\mathcal{C}}(t,t') - \Delta(t,t') \quad (3)$$

and should be determined self-consistently to achieve the equivalence between local and impurity GFs and self-energies ($G_{\text{loc}} = G_{\text{imp}}$, $\Sigma_{\text{loc}} = \Sigma_{\text{imp}}$); $D_0^{-1}(t,t')$ is the inverse of the phonon bare Green's function,

$$D_0^{-1}(t,t') = \frac{-\partial_t^2 - \omega_0^2}{2\omega_0} \delta_{\mathcal{C}}(t,t'); \quad (4)$$

all functions in (2) are matrices 2×2 and $\delta_{\mathcal{C}}(t,t')$ is delta function defined on $\mathcal{C}$.

For Bethe lattice

$$\mathcal{G}_0^{-1} = i\omega_n + \mu - t_{\parallel}^2 G_{\text{loc}}, \quad (5)$$

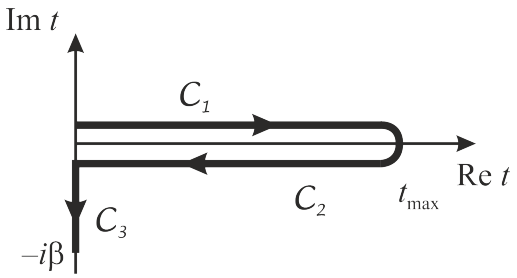

FIG. 2. Kadanoff–Baym contour with three time domains: real-time forward $\mathcal{C}_1$ and backward $\mathcal{C}_2$, and imaginary-time $\mathcal{C}_3$. The arrows set the contour time ordering; $t_{\max}$ corresponds to the maximum real-time propagation of the solution.

and, taking into account the equivalence of the sites of the dimer,

$$\mathcal{G}_0 = \begin{pmatrix} \mathcal{G}_{11} & \mathcal{G}_{12} \\ \mathcal{G}_{12} & \mathcal{G}_{11} \end{pmatrix}, \tag{6}$$

$$\mathcal{G}_{11} = \frac{1}{2}\left[G_{\mathrm{B}}(i\omega_n + \mu - t_\perp) + G_{\mathrm{B}}(i\omega_n + \mu + t_\perp)\right], \tag{7}$$

$$\mathcal{G}_{12} = \frac{1}{2}\left[G_{\mathrm{B}}(i\omega_n + \mu - t_\perp) - G_{\mathrm{B}}(i\omega_n + \mu + t_\perp)\right], \tag{8}$$

$$G_{\mathrm{B}}(\xi) = \frac{1}{2t_\parallel^2}\left(\xi - \sqrt{\xi^2 - 4t_\parallel^2}\right). \tag{9}$$

The Dyson equations for the impurity problem are

$$\left[i\partial_t - \epsilon(t)\right] G(t,t') - \int_{\mathcal{C}} d\bar{t}\, \tilde{\Sigma}(\bar{t},t) G(t,\bar{t}) = \delta_{\mathcal{C}}(t,t'), \tag{10}$$

$$D(t,t') = D_0(t,t') + \int_{\mathcal{C}} d\bar{t} d\bar{\bar{t}}\, D_0(t,\bar{t}) \Pi(\bar{t},\bar{\bar{t}}) D(\bar{\bar{t}},t'), \tag{11}$$

where $\epsilon(t)$ is the one-particle Hamiltonian,

$$\epsilon(t) = \begin{pmatrix} \mu + \Sigma_1^{\mathrm{MF}} & -t_\perp \\ -t_\perp & \mu + \Sigma_2^{\mathrm{MF}} \end{pmatrix} \tag{12}$$

with the mean-field contribution

$$\Sigma_i^{\mathrm{MF}}(t) = g X_i(t). \tag{13}$$

The impurity self-energy for electrons includes two components,

$$\tilde{\Sigma} = \Sigma_{\mathrm{ME}} + \Delta; \tag{14}$$

where the hybridization function $\Delta(t,t')$ in the case of the Bethe lattice has the form

$$\Delta(t,t') = t_\parallel^2 G(t,t'), \tag{15}$$

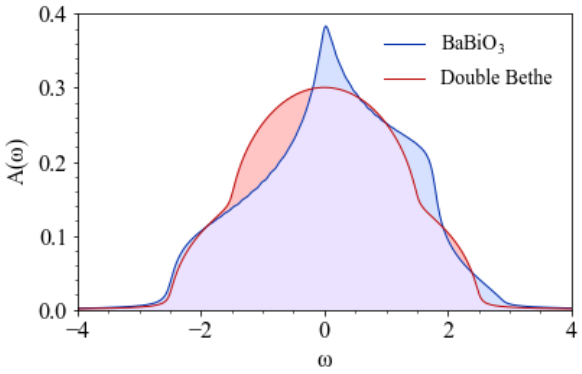

FIG. 3. The density of electron states for the tight-binding model of $BaBiO_3$ compounds from [41] and for the double Bethe lattice model used in this work. $t_\parallel = 1.0; t_\perp = 0.5; g = 0.43$.

and Σ_{ME} is the beyond-mean-field contribution to the self-energy, which in terms of the self-consistent Migdal approximation is [39, 40]:

$$\Sigma_{\mathrm{ME}}(t,t') = ig^2 D(t,t') G(t,t'); \tag{16}$$

the impurity self-energy for phonons whithin this approximation reads

$$\Pi(t,t') \to \Pi_{\mathrm{ME}}(t,t') = -2ig^2 G(t,t') G(t',t). \tag{17}$$

III. METHOD

[Contour equations]
[NESSi and extentions]
To solve the Dyson equations (10–11), a set of minimum four components defined on different time domains of the KB contour is needed for both electron and phonon GFs. In this work, we use the lesser $G^<$, the retarded G^R, the left-mixing $G^\rceil$, and Matsubara G^M components and solve the equations with the help of *Non-Equilibrium Systems Simulation Library* (Nessi, [42]).

The laser pulse was modelled via Peierls substitution,

$$t_\perp \to t_\perp(t) = t_\perp e^{iA(t)}, \tag{18}$$

where the vector potential of the pump is

$$A(t) = \frac{A}{\tau} e^{-t^2/2\tau^2} \cos(\omega t) \tag{19}$$

with A, τ and ω are the amplitude, pulse width, and frequency of the vector potential, respectively.

IV. RESULTS

[Equilibrium; without laser - bipolar state? - phase diagram]

[Excitation]

[1) two identical sites?]

[2) different chemical potential on sites - modeling of distorted structure of BaBiO?]

[3) various e-ph couplings?]

V. CONCLUSIONS

Blablabla

ACKNOWLEDGEMENTS

The work was supported by Russian Found for Basic Research (Project No. 18-02-40001 mega).

[1] A. Sleight, J. Gillson, and P. Bierstedt, High-temperature superconductivity in the bapb1-xbixo3 systems, Solid State Communications **17**, 27 (1975).

[2] L. F. Mattheiss, E. M. Gyorgy, and D. W. Johnson, Superconductivity above 20 k in the ba-k-bi-o system, Phys. Rev. B **37**, 3745 (1988).

[3] A. W. Sleight, Bismuthates: Babio3 and related superconducting phases, Physica C: Superconductivity and its Applications **514**, 152 (2015), superconducting Materials: Conventional, Unconventional and Undetermined.

[4] J. F. Federici, B. I. Greene, E. H. Hartford, and E. S. Hellman, Optical characterization of excited states in $babio_3$, Phys. Rev. B **42**, 923 (1990).

[5] C. M. Varma, Missing valence states, diamagnetic insulators, and superconductors, Phys. Rev. Lett. **61**, 2713 (1988).

[6] I. Haseand T. Yanagisawa, Madelung energy of the valence-skipping compound $BaBio_3$, Phys. Rev. B **76**, 174103 (2007).

[7] S. Uchida, K. Kitazawa, and S. Tanaka, Superconductivity and metal-semiconductor transition in BaPb1-xBixO3, Phase Transitions **8**, 95 (1987).

[8] N. C. Plumb, D. J. Gawryluk, Y. Wang, Z. Ristić, J. Park, B. Q. Lv, Z. Wang, C. E. Matt, N. Xu, T. Shang, K. Conder, J. Mesot, S. Johnston, M. Shi, and M. Radović, Momentum-resolved electronic structure of the high-T_c superconductor parent compound $babio_3$, Phys. Rev. Lett. **117**, 037002 (2016).

[9] S. Balandeh, R. J. Green, K. Foyevtsova, S. Chi, O. Foyevtsov, F. Li, and G. A. Sawatzky, Experimental and theoretical study of the electronic structure of single-crystal $babio_3$, Phys. Rev. B **96**, 165127 (2017).

[10] M. Qvarford, V. G. Nazin, A. A. Zakharov, M. N. Mikheeva, J. N. Andersen, M. K. J. Johansson, G. Chiaia, T. Rogelet, S. Söderholm, O. Tjernberg, H. Nylén, I. Lindau, R. Nyholm, U. O. Karlsson, S. N. Barilo, and S. V. Shiryaev, Photoemission and x-ray absorption study of superconducting and semiconducting $ba_{1-x}k_xBio_3$ single crystals, Phys. Rev. B **54**, 6700 (1996).

[11] A. P. Menushenkov, K. V. Klementev, A. V. Kuznetsov, and M. Y. Kagan, Superconductivity in ba1-x KxBiO3: Possible scenario of spatially separated fermi-bose mixture, Journal of Experimental and Theoretical Physics **93**, 615 (2001).

[12] A. Menushenkov, K. Klementev, A. Kuznetsov, and M. Kagan, An interplay between spatially separated fermi and bose subsystems and superconductivity in perovskite-like oxides, Physica B: Condensed Matter **312-313**, 31 (2002).

[13] A. P. Menushenkov, A. V. Kuznetsov, K. V. Klementiev, and M. Y. Kagan, Fermi-bose mixture in ba(k)BiO3 superconducting oxide, Journal of Superconductivity and Novel Magnetism **29**, 701 (2016).

[14] A. P. Menushenkov, K. V. Klement'ev, P. V. Konarev, and A. A. Meshkov, Anharmonicity and superconductivity in ba0.6k0.4bio3, Journal of Experimental and Theoretical Physics Letters **67**, 1034 (1998).

[15] A. P. Menushenkovand K. V. Klementev, Extended x-ray absorption fine-structure indication of a double-well potential for oxygen vibration in ba1 -xKxBiO3, Journal of Physics: Condensed Matter **12**, 3767 (2000).

[16] C. L. Smallwood, R. A. Kaindl, and A. Lanzara, Ultrafast angle-resolved photoemission spectroscopy of quantum materials, EPL (Europhysics Letters) **115**, 27001 (2016).

[17] M. Buzzi, M. Först, R. Mankowsky, and A. Cavalleri, Probing dynamics in quantum materials with femtosecond x-rays, Nature Reviews Materials **3**, 299 (2018).

[18] J. Graf, C. Jozwiak, C. L. Smallwood, H. Eisaki, R. A. Kaindl, D.-H. Lee, and A. Lanzara, Nodal quasiparticle meltdown in ultrahigh-resolution pump–probe angle-resolved photoemission, Nature Physics **7**, 805 (2011).

[19] C. L. Smallwood, J. P. Hinton, C. Jozwiak, W. Zhang, J. D. Koralek, H. Eisaki, D.-H. Lee, J. Orenstein, and A. Lanzara, Tracking cooper pairs in a cuprate superconductor by ultrafast angle-resolved photoemission, Science **336**, 1137 (2012).

[20] S.-L. Yang, J. Sobota, D. Leuenberger, Y. He, M. Hashimoto, D. Lu, H. Eisaki, P. Kirchmann, and Z.-X. Shen, Inequivalence of single-particle and population lifetimes in a cuprate superconductor, Physical Review Letters **114**, 10.1103/physrevlett.114.247001 (2015).

[21] W. Zhang, T. Miller, C. L. Smallwood, Y. Yoshida, H. Eisaki, R. A. Kaindl, D.-H. Lee, and A. Lanzara, Stimulated emission of cooper pairs in a high-temperature cuprate superconductor, Scientific Reports **6**, 10.1038/srep29100 (2016).

[22] Y. Ishida, T. Saitoh, T. Mochiku, T. Nakane, K. Hirata, and S. Shin, Quasi-particles ultrafastly releasing kink bosons to form fermi arcs in a cuprate superconductor, Scientific Reports **6**, 10.1038/srep18747 (2016).

[23] C. L. Smallwood, W. Zhang, T. L. Miller, G. Affeldt, K. Kurashima, C. Jozwiak, T. Noji, Y. Koike, H. Eisaki, D.-H. Lee, R. A. Kaindl, and A. Lanzara, Influence of optically quenched superconductivity on quasiparticle relaxation rates inBi2sr2cacu2o8, Physical Review B **92**, 10.1103/physrevb.92.161102 (2015).

[24] C. L. Smallwood, W. Zhang, T. L. Miller, C. Jozwiak, H. Eisaki, D.-H. Lee, and A. Lanzara, Time- and momentum-resolved gap dynamics inBi2sr2cacu2o8, Physical Review B **89**, 10.1103/physrevb.89.115126 (2014).

[25] W. Hu, S. Kaiser, D. Nicoletti, C. R. Hunt, I. Gierz, M. C. Hoffmann, M. L. Tacon, T. Loew, B. Keimer, and A. Cavalleri, Optically enhanced coherent transport in YBa2cu3o6.5 by ultrafast redistribution of interlayer coupling, Nature Materials **13**, 705 (2014).

[26] L. Rettig, R. Cortés, S. Thirupathaiah, P. Gegenwart, H. S. Jeevan, M. Wolf, J. Fink, and U. Bovensiepen, Ultrafast momentum-dependent response of electrons in AntiferromagneticEuFe2as2driven by optical excitation, Physical Review Letters **108**, 10.1103/physrevlett.108.097002 (2012).

[27] L. Rettig, R. Cortés, H. S. Jeevan, P. Gegenwart, T. Wolf, J. Fink, and U. Bovensiepen, Electron–phonon coupling in 122 fe pnictides analyzed by femtosecond time-resolved photoemission, New Journal of Physics **15**, 083023 (2013).

[28] A. Pogrebna, T. Mertelj, N. Vujičić, G. Cao, Z. A. Xu, and D. Mihailovic, Coexistence of ferromagnetism and superconductivity in iron based pnictides: a time resolved magnetooptical study, Scientific Reports **5**, 10.1038/srep07754 (2015).

[29] M. Naseska, A. Pogrebna, G. Cao, Z. A. Xu, D. Mihailovic, and T. Mertelj, Ultrafast destruction and recovery of the spin density wave order in iron-based pnictides: A multipulse optical study, Physical Review B **98**, 10.1103/physrevb.98.035148 (2018).

[30] H. Schäfer, V. V. Kabanov, M. Beyer, K. Biljakovic, and J. Demsar, Disentanglement of the electronic and lattice parts of the order parameter in a 1d charge density wave system probed by femtosecond spectroscopy, Physical Review Letters **105**, 10.1103/physrevlett.105.066402 (2010).

[31] H. Schaefer, V. V. Kabanov, and J. Demsar, Collective modes in quasi-one-dimensional charge-density wave systems probed by femtosecond time-resolved optical studies, Physical Review B **89**, 10.1103/physrevb.89.045106 (2014).

[32] T. Rohwer, S. Hellmann, M. Wiesenmayer, C. Sohrt, A. Stange, B. Slomski, A. Carr, Y. Liu, L. M. Avila, M. Kalläne, S. Mathias, L. Kipp, K. Rossnagel, and M. Bauer, Collapse of long-range charge order tracked by time-resolved photoemission at high momenta, Nature **471**, 490 (2011).

[33] S. Hellmann, T. Rohwer, M. Kalläne, K. Hanff, C. Sohrt, A. Stange, A. Carr, M. Murnane, H. Kapteyn, L. Kipp, M. Bauer, and K. Rossnagel, Time-domain classification of charge-density-wave insulators, Nature Communications **3**, 10.1038/ncomms2078 (2012).

[34] C. Laulhé, T. Huber, G. Lantz, A. Ferrer, S. Mariager, S. Grübel, J. Rittmann, J. Johnson, V. Esposito, A. Lübcke, L. Huber, M. Kubli, M. Savoini, V. Jacques, L. Cario, B. Corraze, E. Janod, G. Ingold, P. Beaud, S. Johnson, and S. Ravy, Ultrafast formation of a charge density wave state in 1t-TaS2 : Observation at nanometer scales using time-resolved x-ray diffraction, Physical Review Letters **118**, 10.1103/physrevlett.118.247401 (2017).

[35] J. Zhang, C. Lian, M. Guan, W. Ma, H. Fu, H. Guo, and S. Meng, Photoexcitation induced quantum dynamics of charge density wave and emergence of a collective mode in 1t-TaS2, Nano Letters **19**, 6027 (2019).

[36] A. Zong, A. Kogar, Y.-Q. Bie, T. Rohwer, C. Lee, E. Baldini, E. Ergeçen, M. B. Yilmaz, B. Freelon, E. J. Sie, H. Zhou, J. Straquadine, P. Walmsley, P. E. Dolgirev, A. V. Rozhkov, I. R. Fisher, P. Jarillo-Herrero, B. V. Fine, and N. Gedik, Evidence for topological defects in a photoinduced phase transition, Nature Physics **15**, 27 (2018).

[37] D. Nicoletti, E. Casandruc, D. Fu, P. Giraldo-Gallo, I. R. Fisher, and A. Cavalleri, Anomalous relaxation kinetics and charge-density-wave correlations in underdoped BaPb1-xBixO3, Proceedings of the National Academy of Sciences **114**, 9020 (2017).

[38] A. Georges, G. Kotliar, W. Krauth, and M. J. Rozenberg, Dynamical mean-field theory of strongly correlated fermion systems and the limit of infinite dimensions, Reviews of Modern Physics **68**, 13 (1996).

[39] Y. Murakami, P. Werner, N. Tsuji, and H. Aoki, Interaction quench in the holstein model: Thermalization crossover from electron- to phonon-dominated relaxation, Physical Review B **91**, 10.1103/physrevb.91.045128 (2015).

[40] Y. Murakami, P. Werner, N. Tsuji, and H. Aoki, Multiple amplitude modes in strongly coupled phonon-mediated superconductors, Physical Review B **93**, 10.1103/physrevb.93.094509 (2016).

[41] A. Khazraie, K. Foyevtsova, I. Elfimov, and G. A. Sawatzky, Oxygen holes and hybridization in the bismuthates, Physical Review B **97**, 10.1103/physrevb.97.075103 (2018).

[42] M. Schüler, D. Golež, Y. Murakami, N. Bittner, A. Hermann, H. U. R. Strand, P. Werner, and M. Eckstein, Nessi: The non-equilibrium systems simulation package (2019), arXiv:1911.01211.